INT. J. NUM. METH. HEAT FLUID FLOW, VOL. 5, 301–311 (1995)

NUMERICAL STUDY OF ENHANCED OIL RECOVERY USING SURFACTANTS

A. CHATTERJEE AND K. MURALIDHAR

Department of Mechanical Engineering, Indian Institute of Technology, Kanpur 208016, India

ABSTRACT

The analysis of enhanced oil recovery using surfactants is presented here. Surfactants lower the surface tension between oil and water and hence the capillary resistance to flow. The mathematical description of this problem requires modelling of multi-phase flow in a porous medium. A pressure-based formulation has been used in the present study. The governing partial differential equations have been solved by a finite difference method. Both Newtonian and non-Newtonian (shear thinning) behaviour of oil are considered. Results clearly show an improvement in oil recovery in the presence of surfactants. A study of the ideal case where surface tension is reduced to zero shows that oil recovery can be very high.

KEY WORDS Enhanced oil recovery Surfactants Numerical simulation Finite differences Shear-thinning fluids

NOMENCLATURE

C	tortuosity factor,
H	consistency index in Herschel–Bulkley model, Ns^n/m^2,
H_i	phase enthalpy, J/Kg,
K	absolute permeability of the formation, m ,
K_{eff}	absolute permeability of the formation in the presence of shear thinning behaviour of oil, m^2,
K_n	absolute permeability of the formation in the presence of Newtonian behaviour of oil, m^2,
$K_{ro,w}$	relative permeability of oil and water respectively,
L	length of the domain, m,
p_c	capillary pressure between oil and water phases, N/m^2,
$p_{o,w}$	phase pressure of oil and water respectively, N/m^2,
$p_{1,2}$	absolute pressures on injection and exit planes, N/m^2,
p_1	absolute pressure at oil–water interface, N/m^2,
ppv	percentage pore volume of oil recovery,
$Q_{o,w}$	mass sources for oil and water,
$S_{o,w}$	saturation of oil and water in the porous region,
t, Δt	time and time step, s,
T	temperature, °C,
T_f	temperature of rock formation,
x, y	Cartesian coordinates, m,
Δx, Δy	grid size along x and y axis respectively, m.

Greek symbols

β	expansivity, $°C^{-1}$,
ξ	compressibility, Pa^{-1},
μ	dynamic viscosity of the fluid phase, N m/s,
ε	Porosity.

Superscript

n	current time step.

Subscript

i, j	node indices along x and y axis respectively.

0961–5539/95/040301–11$2.00

Received July 1993
Revised March 1994

INTRODUCTION

Oil is trapped in the microscopic pores of the earth's crust and will flow only when large pressure differences are applied. The pores are tortuous, interconnected and irregular. Resistance to flow of hydrocarbons in these pores arises from both viscous and capillary effects. Surfactants can be used to lower the capillary resistance to flow.

As early as 1927, Uren and Fahmy[1] concluded that an inverse relationship exists between oil–water interface tension and the percentage of oil recovered by water-flooding. Since then the necessity of reducing the interfacial tension between oil and the flooding medium was realised and the importance of surfactants is now well established.

Surfactants are surface active chemicals mixed with the injected water that reduce interfacial tension between oil and water. This leads to a considerable reduction in capillary forces and a consequent increase in the recovery of oil. In the present study oil production for the following three problems have been compared against one another: (1) oil extraction without surfactants; (2) extraction with the partially effective surfactant; (3) the ideal case when capillary resistance is zero.

The third problem represents the absolute maximum oil recovery that is possible in the absence of surface tension. In all the three problems non-Newtonian behaviour of oil is considered in the analysis. Oil is modelled as a power-law fluid that displays shear thinning behaviour under the influence of large shear stresses. Flow in the porous medium is modelled accordingly using a modified Darcy's law[2]. Oil recovery is seen to increase when shear-thinning is included in the model equations.

FORMULATION

The physical model used in the present study is shown in *Figure 1*. The flow is two dimensional and we solve for the oil and water pressures separately. The differences between the two pressures is a measure of the surface tension. This results in a complete two phase model of flow occurring in a porous region.

Equations governing velocity and pressure are as follows[3,4]:

(1) conservation of mass of both oil and water phases;
(2) modified Darcy's law that includes the capillary as well as viscous resistance and shear thinning behaviour of the oil phase;
(3) constitutive relations that supply information about the capillary pressure and the non-Newtonian behaviour of the fluids involved;
(4) equations of state for oil and water properties as a function of temperature.

These equations can be combined to generate a set of two coupled, non-linear partial differential equations for the oil and water phase pressures. These equations must be solved subject to suitable initial and boundary conditions. The mathematical model predicts the movement of

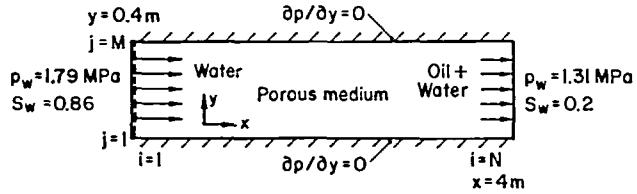

Figure 1 Flow configuration and coordinate system

the water front from the inflow plane into the oil-rich porous region. This increase in water saturation is a measure of the amount of oil displaced. Oil displacement is measured in terms of the percentage pore volume (*ppv*). *ppv* is the ratio of the total volume of oil produced and the total pore volume of the porous medium.

MATHEMATICAL MODEL

The mass balance equations in the oil and water phases are jointly writeen as[3]:

$$\frac{\partial}{\partial t}(\varepsilon S_i \rho_i) + \nabla \cdot \mathbf{u}_i \rho_i = Q_i \tag{1}$$

where t is time, ∇ is the gradient operator, $\mathbf{u}$ is the velocity vector, ρ is density, S is saturation and ε is porosity. Index i refers individually to the oil phase and the water phase. In a two phase flow problem we require $\sum S_i = 1$. Q is mass source term for the appropriate phase and has been taken to be zero in the present study. The momentum equation is expressed in the form of a modified Darcy's law:

$$\mathbf{u}_i = -\frac{K(\nabla p_i) K_{ri}(p_c)}{\mu_i} \nabla p_i \tag{2a}$$

Here K is the absolute permeability of the oil-rich rock formation, K_r is the relative permeability, μ is viscosity and p_i is the phase pressure. In general both oil and water containing surfactants can exhibit non-Newtonian behaviour and hence K is a function of the local pressure gradient. In the present work the surfactant solution is assumed to retain Newtonian behaviour. The relative permeability depends on p_c, the local capillary pressure. The capillary pressure prevents equalization of the phase pressures and hence, $p_c = p_{\text{oil}} - p_{\text{water}}$ is non-zero.

Oil trapped in the pores of the earth can also display viscoplastic behaviour. In such problems (2a) is modified to the form:

$$\begin{aligned} \mathbf{u}_i &= \frac{-K K_{ri}(p_c)}{\mu_i}\left[\nabla \mathrm{p}_i - G_i(p_c)\frac{\nabla \mathrm{p}_i}{|\nabla \mathrm{p}_i|}\right] \quad \text{if} \quad |\nabla \mathrm{p}_i| > G_i \\ &= 0, \qquad\qquad\qquad\qquad\qquad\qquad \text{otherwise} \end{aligned} \tag{2b}$$

Here G_i is a constant and is zero for Newtonian fluids. It is the threshold pressure gradient below which there is no flow.

The shear thinning behaviour of oil is well-described by the Herschel–Bulkley model[2]. In this model the appropriate form of K in (2a) for the oil phase is given as:

$$K_{\text{eff}} = \mu_0 \left(\frac{K_n}{\mu_{\text{eff}}}\right)^{1/n} |\nabla \mathrm{p}_0|^{(1/n-1)} \tag{2c}$$

Here K_n is the absolute permeability of the formation in the absence of non-Newtonian behaviour and μ_{eff} is given as:

$$\mu_{\text{eff}} = \frac{H}{4}\left(3 + \frac{1}{n}\right)^n (8C\varepsilon K_n)^{(1-n)/2} \tag{2d}$$

In the above equation H is the consistency index of the Herschel–Bulkley model and n is the flow behaviour index equivalent to the index in power law fluid. C is the tortuosity factor of the formation. Based on the data presented in Reference 2, C is taken as 25/12 in this study. Equation (2d) reduces to the Newtonian case of $\mu_{\text{eff}} = H = \mu_0$ and $K_{\text{eff}} = K_n$ for $n = 1$.

Non-Newtonian behaviour can be further complicated by variations in surfactant concentrations in the fluid phase. This effect can be modelled by writing a transport equation

for concentration that accounts for advection and diffusion. This has not been accounted for in the present calculations.

If the injected water temperature is different from the formation temperature (1) and (2) must be supplemented with the energy equation. Temperature variations significantly affect fluid properties and hence the oil recovery. The energy equation determines the temperature field and is written as:

$$\frac{\partial}{\partial t}\left[\varepsilon \sum_i S_i \rho_i H_i + (1-\varepsilon) H_{\text{rock}}\right] + \nabla \cdot \left(\sum_i \mathbf{u}_i S_i H_i\right) = \nabla \cdot k \nabla T \tag{3}$$

In (3), T is the local volume-averaged temperature, H_i is the phase enthalpy and k is the composite thermal conductivity.

In (1), (2) and (3) one can view the phase pressures p_i and temperature T as the dependent variables. All other quantities are supplied in the form of equations of state. These equations are stated below:

$$H_i = C_i T_i \xi_i = \frac{1}{\rho_i}\frac{\partial \rho_i}{\partial p_i}\bigg|_T$$
$$\beta_i = -\frac{1}{\rho_i}\frac{\partial \rho_i}{\partial T}\bigg|_{p_i} \qquad \text{and} \qquad \mu_i = \mu_i(T) \tag{4}$$

Typical values of parameters appearing in (4) are taken from Reference 5 and summarized in *Table 1*. The expressions related to unsaturated flow namely, $K_{ri} = K_{ri}(S_w)$ and $p_c = p_c(S_w)$ are shown in *Figure 2*. Since $\sum S_i = 1$ the functional relationship can be shown in terms of water or oil saturation alone. In the present study results have been obtained in terms of the water saturation. An increase in water saturation with time clearly shows oil displacement.

In *Figure 2*, curve (a) shows relative permeability as a function of saturation when the injected water is free of surfactants. Curve (b) shows this relationship in the presence of dissolved surfactants. Normal concentrations of these additions are small enough to keep the density of water unchanged[6]. Case (c) referred to in *Figure 2* corresponds to the ideal case when capillary resistance has been reduced to zero.

It must be pointed out at this stage that the formulation of the oil recovery problem can alternatively be carried out in terms of water saturation and one of the phase pressures as the dependent variables. The water saturation equation is of the advection–diffusion type. Hence, under certain conditions, this approach can lead to difficulties in numerical computation of the water saturation since the water–oil interface can be quite sharp. In contrast to this the pressure field is governed by a diffusion-like equation and must be continuous everywhere. This guarantees an improvement in the accuracy of the numerical simulation as higher order finite difference

Table 1 Properties used in numerical calculation

Absolute permeability, $K = 132$ Darcies
Porosity, $\varepsilon = 0.375$
Compressibility: oil, $\xi_o = 0.03447\ \text{Pa}^{-1}$, water, $\xi_w = 0.02137\ \text{Pa}^{-1}$
In situ formation pressure = 1.31 Mpa
Injection pressure = 1.793 Mpa

Dynamic viscosity (Pa s):

	20°C	40°C	60°C	80°C
Oil	4.12	2.37	0.61	0.10
Water	1.03×10^{-3}	6.6×10^{-4}	4.73×10^{-4}	3.67×10^{-4}

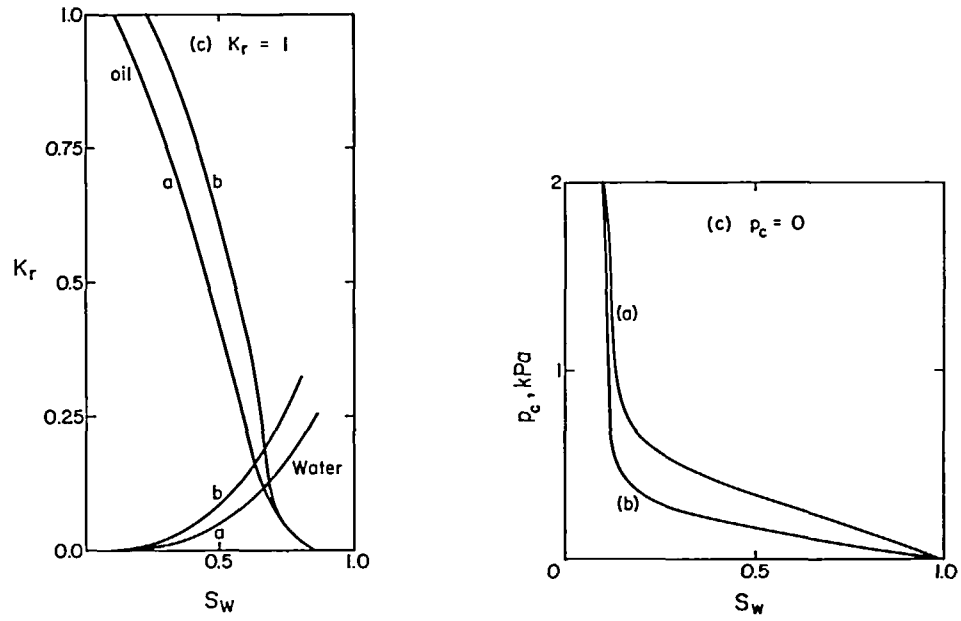

Figure 2 (a) Relative permeability as a function of saturation. (b) Capillary pressure as a function of saturation

methods are used on a refined mesh. For this reason, oil and water pressures have been used as the primary dependent variables in the present work.

The pressure and temperature equations derived from (1)–(4) can be shown to be the following:

$$-S_i\beta_i\frac{\partial T}{\partial t}+S_i\xi_i\frac{\partial p_i}{\partial t}+\text{sgn}\frac{dS_w}{dp_c}\left[\frac{\partial}{\partial t}(p_o-p_w)\right]=\frac{1}{\rho_i}\nabla\cdot\frac{(KK_{ri}\rho_i)}{\mu_i}\nabla p_i+\frac{Q_i}{\varepsilon\rho_i} \tag{5}$$

$$\frac{\partial T}{\partial t}+\mathbf{U}\cdot\nabla T=\frac{k}{\sigma_T}\nabla^2 T \tag{6}$$

In (5), sgn = 1 for water and −1 for oil. In (6),

$$\mathbf{U}=\frac{1}{\sigma_T}\sum\rho_i C_i\mathbf{u} \qquad \text{and} \qquad \sigma_T=\varepsilon\left\{\sum_i S_i\rho_i C_i\right\}+(1-\varepsilon)(\rho C)_{\text{rock}}$$

The present study examines the role of surfactants in improving oil recovery and the effect of shear thinning behaviour of oil. Accordingly we assume the formation temperature to be prescribed and equal to the injection water temperature. Equation (5) is solved on a rectangular domain subject to a quiescent initial condition, impermeable confining walls and specified water and oil pressures on the inflow and outflow planes of the physical domain. These conditions are shown schematically in *Figure 1*.

The use of Dirichlet boundary condition on the outflow plane is justified only if the location of this plane is far away from the region effected by water injection. In the present work oil recovery is computed over a distance of 2 m and the outflow plane is located at a distance of 4 m from the inflow plane. For the time period of three hours considered in the present simulation the water front moves a distance of approximately 1 m. Numerical experiments show that oil recovery is insensitive to the location of the outflow plane.

NUMERICAL SOLUTION

The oil and water pressure equations arising from (5) are strongly coupled and non-linear. They have been solved using a control-volume finite difference method. The difference equations are solved simultaneously to extract the fluid pressures. Central differencing is used for the spatial derivatives and time marching proceeds via a fully implicit scheme. Hence the numerical procedure is unconditionally stable with respect to the time step. Interfacial property values falling on the control surface are evaluated as the harmonic average of neighbouring nodal values. Since the equations are non-linear Picard iterations are used within each time step to obtain a converged solution.

The finite difference forms of (5) are given below. The oil and water temperatures are assumed to be equal in this development. Here Δx and Δy define a Cartesian mesh and Δt is the time step. A grid size of $\Delta x = 0.05$ m and $\Delta y = 0.2$ m is used. The time step varies from 0.001 h at small time to 0.02 h at larger times. A convergence criterion of 0.01 (maximum relative change of pressure at any node in each iteration) is imposed. Convergence is monotonically attained and hence no under-relaxation is used. The current time level is represented by n and the future time by $n + 1$.

Oil

$$[A_o p_{o_{i+1,j}} + B_o p_{o_{i,j}} + C_o p_{w_{i,j}} + D_o p_{o_{i-1,j}} + E_{o_i} p_{o_{j+1}} + F_o p_{o_{i,j-1}}]^{n+1} = G_o^{n+1} \tag{7a}$$

Water

$$[A_w p_{w_{i+1,j}} + B_w p_{w_{i,j}} + C_w p_{o_{i,j}} + D_w p_{w_{i-1,j}} + E_w p_{w_{i,j+1}} + F_w p_{w_{i,j-1}}]^{n+1} = G_w^{n+1} \tag{7b}$$

The coefficients $A_o, B_o, \ldots, F_w, G_w$ are given as:

Equation (7a)

$$A_o = -\left\{\frac{\theta_e}{\rho_o(\Delta x)^2}\right\}_{i,j}^{n+1}$$

$$B_o = \left[\frac{S_o\xi_o - \left(\frac{dS_w}{dp_c}\right)}{\Delta t} + \frac{1}{\rho_o}\left\{\frac{\theta_e + \theta_w}{(\Delta x)^2} + \frac{\theta_n + \theta_s}{(\Delta y)^2}\right\}_{i,j}\right]^{n+1}$$

$$C_o = \left\{\frac{dS_w}{dp_c}\right\}_{i,j}^{n+1} \frac{1}{\Delta t} \qquad D_o = -\left\{\frac{\theta_w}{\rho_o(\Delta x)^2}\right\}_{i,j}^{n+1}$$

$$F_o = -\left\{\frac{\theta_s}{\rho_o(\Delta y)^2}\right\}_{i,j}^{n+1}$$

$$G_o\left[\left\{\frac{S_o\xi_o - \frac{dS_w}{dp_c}}{\Delta t}\right\}^{n+1} \cdot p_o^n + \frac{1}{\Delta t}\left\{\frac{dS_w}{dp_c}\right\}^{n+1} p_w^n + \frac{Q_o^{n+1}}{\varepsilon\rho_o}\right]_{i,j}$$

Equation(7b)

$$A_w = -\left\{\frac{\gamma_e}{\rho_w(\Delta x)^2}\right\}_{i,j}^{n+1}$$

$$B_w = \left[\frac{S_w\xi_w - \left(\frac{dS_w}{dp_c}\right)}{\Delta t} + \frac{1}{\rho_w}\left\{\frac{\gamma_e+\gamma_w}{(\Delta x)^2} + \frac{\gamma_n+\gamma_s}{(\Delta y)^2}\right\}\right]_{i,j}^{n+1}$$

$$C_w = \left\{\frac{dS_w}{dp_c}\right\}_{i,j}^{n+1}\frac{1}{\Delta t}$$

$$D_w = -\left\{\frac{\gamma_w}{\rho_w(\Delta x)^2}\right\}_{i,j}^{n+1} \qquad E_w = -\left\{\frac{\gamma_s}{\rho_w(\Delta y)^2}\right\}_{i,j}^{n+1}$$

$$F_w = -\left\{\frac{\gamma_s}{\rho_w(\Delta y)^2}\right\}_{i,j}^{n+1}$$

$$G_w = \left[\left\{\frac{S_w\xi_w - \frac{dS_w}{dp_c}}{\Delta t}\right\}^{n+1} p_w^n + \frac{1}{\Delta t}\left\{\frac{dS_w}{dp_c}\right\}^{n+1} p_o^n + \frac{Q_w^{n+1}}{\varepsilon\rho_w}\right]_{i,j}$$

Here $\theta = KK_{ro}\rho_o/\varepsilon\mu_o$ and $\gamma = KK_{rw}\rho_w/\varepsilon\mu_w$.

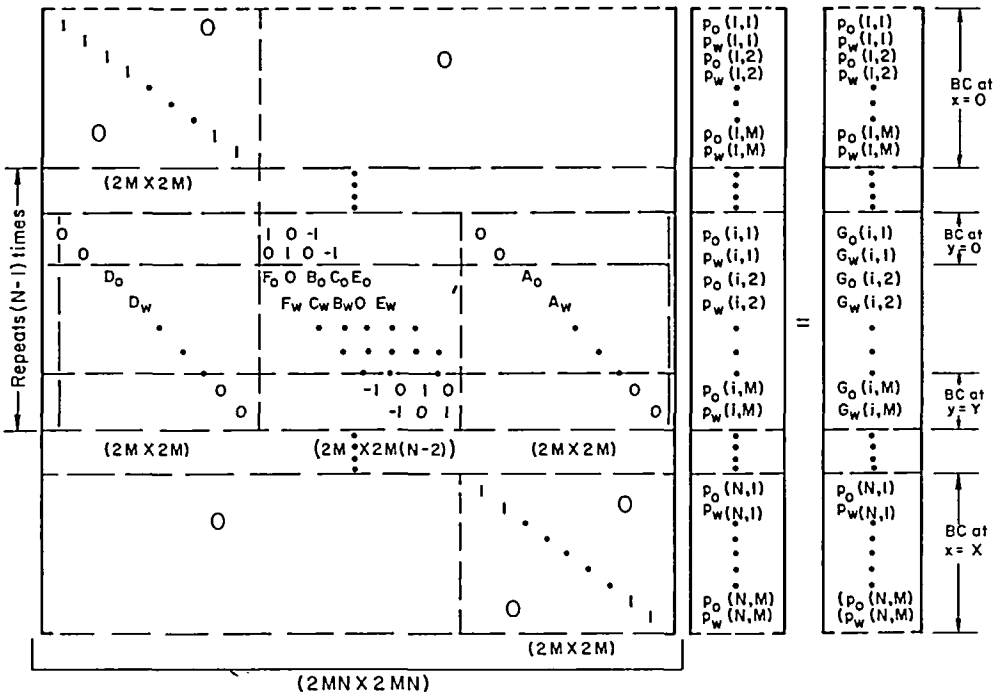

Figure 3 Matrix structure in pressure calculation

In expressions for the coefficients $A, B, \ldots, G$ given above, the suffixes e, w, n, and s stand for the locations midway between $(i, i+1)$, $(i, i-1)$, $(j, j+1)$ and $(j, j-1)$ respectively. The corresponding properties are calculated as the harmonic average of their values prevailing at the nearest nodes. For example, γ_e = harmonic average of $(\gamma(i+1), \gamma(i))$. The matrix structure arising from (7a) and (7b) are shown in *Figure 3*. The matrix so obtained is banded and sparse. A sparse matrix inverter[7] is used in the present work to simultaneously solve for the oil and water pressures.

The finite difference algorithm developed here has been used to solve the system of coupled equations,

$$\nabla \cdot K_o \nabla P_o = 0$$

$$\nabla \cdot K_w \nabla P_w = 0$$

for a known form of distributions of K_o and K_w. The numerical results for this problem compare very well with the analytical solution. The finite difference algorithm presented above has also been used to study the simulation of oil recovery using hot water injection[8].

A Newton–Raphson scheme for the non-linear iterations has also been tried in the present work. One of the principal difficulties while using this method is the computation of derivatives such as dS_w/dp_c from the constitutive relations. These relations are in the form of raw data and because of the possibility of large changes in a variable especially at low water saturation, the derivative calculation becomes inaccurate. Experience gained in the present study shows the need for very small time steps or the use of small relaxation factors. In either case the computational effort with the Newton–Raphson scheme is larger than with Picard iterations.

ALGORITHM

The system of equations governing the distribution of oil and water pressures are non-linear and mutually coupled. They are solved simultaneously and by iteration. As stated earlier, the mass sources have been set equal to zero in the present study. The following procedure has been used to solve for oil and water pressure distributions as functions of time.

(1) The initial distributions of p_o, p_w and S_w at $t = 0$ are prescribed.

(2) The coefficients ($A_o - G_o$ and $A_w - G_w$) of the pressure equations are computed using the values of p_o, p_w and S_w at the current time step and iteration level.

(3) The system of pressure equations is solved to obtain the new values of p_o and p_w at the nodes formed by the grid.

(4) S_w is updated via the constitutive relations using the new pressure values.

(5) Fluid viscosity and compressibility are updated at this stage.

(6) Steps (1)–(5) are repeated until convergence of p_o and p_w is achieved.

(7) Fresh computation is initiated for the next time step starting from step (2).

A three hour simulation typically takes 3 hours of CPU time on a mainframe computer such as HP 9000.

IDEAL CASE

We discuss below the limiting case of an ideal surfactant which when added to the injected water eliminates surface tension altogether. Hence the relative permeability and capillary pressure reach their limiting values of unity and zero respectively. A water front moves through porous medium under these conditions displacing oil completely. In modelling the ideal case we assume that the water saturation in the water phase ahead of the front is at its maximum value, controlled by the irreducible oil saturation. Beyond the front the water saturation is a minimum, equal to the irreducible limit of water saturation. However the relative permeability is unity for water

and oil flow respectively and (2a) simplifies greatly for this problem. The flow resistance arises here from the viscosities of oil and water. For a domain of length L the average oil and water velocities are equal and equal to the speed of movement of the front. For the Newtonian case this speed is estimated from:

$$u = K(p_1 - p_I)/(\mu_w x) = K(p_I - p_2)/(\mu_o(L - x))$$

Here p_1, p_2 and p_I are the injection, exit plane and the interface pressures respectively. x indicates the depth penetrated by the water–oil interface. Eliminating p_I, the expression for the front speed is obtained as:

$$u = \frac{K}{\mu_w \frac{x}{L} + \mu_o\left(1 - \frac{x}{L}\right)} \frac{(p_1 - p_2)}{L} \tag{8}$$

At t = 0, $x = 0$ and at any time t we update x as x(new) = x(old) + $u\Delta t$, where u is calculated from (8) using the old value of x. Oil recovery is measured in terms of *ppv* as $ppv = 100x/L$.

When the shear thinning behaviour of oil is taken into consideration, a closed form solution for u does not exist. In terms of p_1, p_2 and p_I as well as the power-law index n, the modified form of Darcy's law (2a) can be written as:

$$u = \left(\frac{K_n}{\mu_{eff}}\right)^{1/n}\left\{\frac{p_I - p_2}{L - x}\right\}^{1/n} = -\frac{K_n}{\mu_w}\left\{\frac{p_I - p_1}{x}\right\} \tag{9}$$

For each x, (9) is solved for p_I iteratively. With this value of p_I the interface velocity u is calculated as:

$$u = \left(\frac{K_n}{\mu_{eff}}\right)^{1/n}\left\{\frac{p_I - p_2}{L - x}\right\}^{1/n} \tag{10}$$

The same procedure as given after (8) is adopted to obtain x at any time t and finally the *ppv* as a measure of oil recovery.

RESULTS

We present results for the formation shown in *Figure 1*, equations of state $K_r = K_r(S_w)$ and $p_c = p_c(S_w)$ in *Figures 2* and data given in *Table 1*. Oil is modelled as a Newtonian fluid ($n = 1$) as well as a shear thinning fluid ($n < 1$). For the study of shear thinning behaviour of oil, a modified Darcy's law is used (2c) and the value of n as it appears in (2c) is taken to be 0.6. This value of n encompasses a wide variety of crude oils[4]. The formation temperature and the injected water temperature are taken to be equal. Temperature is, however, used as a parameter in the analysis since oil viscosity is a strong function of temperature. The data for *ppv* corresponds to the end of a three hour simulation. Grid refinement studies beyond what was given earlier show no significant change in the results reported here.

The problem of $n = 1$ (Newtonian fluid) for oil is considered first. *Figure 4* shows oil recovery in terms of *ppv* as a function of the formation temperature for the Newtonian behaviour of oil. The three cases, namely injection without surfactants, with surfactants and the ideal case or zero capillary resistance are compared here. The effect of the formation temperature is also visible in this Figure. An increase in the temperature lowers oil viscosity and raises oil recovery. However, the effect of lowering surface tension can be seen to be dramatic in terms of an increase in *ppv*. In particular the comparison between the magnitudes of *ppv* with and without surface tension shows that oil recovery can be improved by nearly a factor of seven.

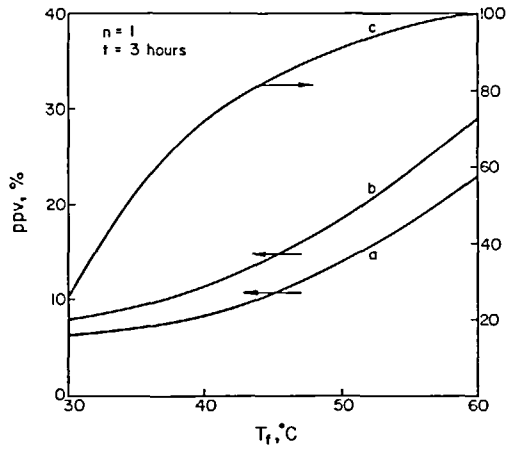

Figure 4 Oil recovery as a function of formation temperature: (a) without surfactants, (b) with surfactants and (c) the ideal case

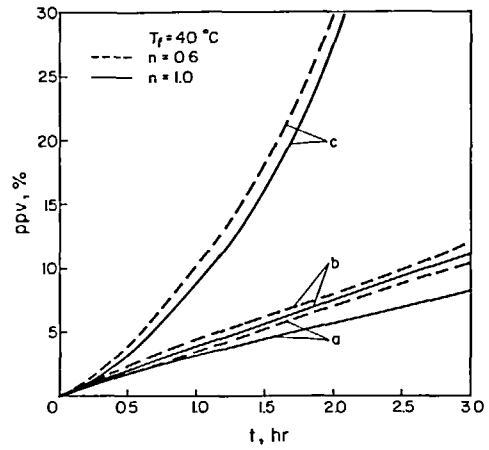

Figure 5 Effect of shear thinning behaviour of oil (a) without surfactants, (b) with surfactants and (c) the ideal case

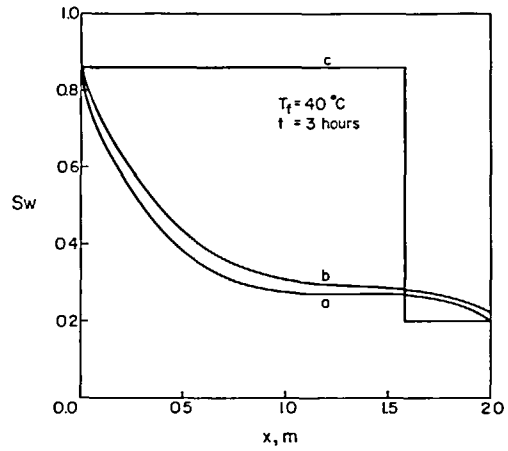

Figure 6 Variation of water saturation with distance at the end of three hours

Figure 5 delineates the effect of shear thinning behaviour of oil. Oil recovery in the presence of shear thinning behaviour is compared with the fact that in the presence of Newtonian behaviour for all the three cases mentioned above. Shear thinning behaviour is characterized by a decrease in the slope of shear stress–shear deformation curve at increasing values of the shear stresses. Accordingly an increase in oil recovery is to be expected and this is shown in *Figure 5*. The extent of increase in *ppv* is small at small times and is progressively higher at larger times. However, in the presence of surfactants the fractional increase in *ppv* for departures of n from unity is small.

Figure 6 compares water saturation profiles after three hours of injection with and without surfactants. It can be seen that water migration is diffuse in case (a) (no surfactant) and case (b) (practical surfactants); however, it moves as a front through the oil-rich region when capillary

resistance is zero (case (c)). Surfactants that show this degree of effectiveness remain to be synthesized.

REFERENCES

1 Uren, L. C. and Fahmy, E. H. *Factors Influencing the Recovery of Petroleum from Unconsolidated Sands by Water Flooding*, AIME, Vol. 318 (1927)
2 Al-Fariss, T. and Pinder, K. L. Flow through porous media of a shear thinning fluid with yield stress, *Can. J. Chem. Eng.*, **65**, 391–405 (1987)
3 Ewing, R. E. (Ed.) *Mathematics of Reservoir Simulation*, SIAM, Philadelphia (1983)
4 Aziz, K. Modeling of thermal oil recovery processes, in *Mathematical and Computational Methods in Seismic Exploration and Reservoir Modeling*, SIAM, Philadelphia (1986)
5 Boberg, T. C. *Thermal Methods of Oil Recovery*, Exxon Monograph, John Wiley, New York (1988)
6 Barenblatt, G. I., Entov, V. M. and Ryzhik, V. M. *Theory of Fluid Flows Through Natural Rocks*, Kluwer, Dordrecht (1990)
7 Duff, I. S. *MA28—A Set of Fortran Subroutines for Sparse Unsymmetric Linear Equations*, AERE Harwell (1980)
8 Pillai, K. M. and Muralidhar, K. A numerical study of oil recovery using water injection method, *Num. Heat Transfer*, (*A*) **24**, 305–322 (1993)